Investigation into the failure of open and filled holes in CFRP laminates under biaxial loading conditions

C. Williamson, J. Cook and A. B. Clarke

QinetiQ Ltd.

ABSTRACT

The use of fibre-reinforced polymer composite materials in the manufacture of structures, from aircraft to racing cars, has increased considerably in recent years. Their specific strength and stiffness permit significant improvements in performance over conventional metallic structures. However, the full commercial and strategic benefits of using structural composites have not been realised because their failure processes are not fully understood, forcing components to be designed with conservative safety factors. Although a large database has been built up for damage growth, resulting from features such as fastener holes (both filled and open) and impact damage, the vast majority of these results have come from uniaxial tests. Unfortunately, despite the reliance of the certification process on results from uniaxial tests, the majority of structures are very rarely loaded uniaxially in service, and little is known about failure under multiaxial loading conditions.

This paper describes the results from an investigation conducted into the failure of a series of carbon fibre reinforced plastic (CFRP) laminates with open and filled holes. A test that was developed to give valid failure data under multiaxial loading conditions using a planar cruciform specimen has been used to experimentally determine the failure envelopes for open and filled holes under the full spectrum of biaxial loading; that is, tension-tension, tension-compression and compression-compression. Four distinct laminates were tested; namely, quasi-isotropic specimens of 2mm and 5mm thickness, manufactured from Ciba T300H/914 carbon-fibre/epoxy material, 2mm thick panels manufactured from a mix of woven and unidirectional T300/914 and 2mm thick specimens manufactures from Fiberite IM7/977-2. Holes were drilled at the centre of the specimens. These were either left open or filled with bolts, either finger-tightened or tightened to a torque of 6Nm. Valid results have been obtained for the materials up to the initiation of failure across the full spectrum of strain ratios. This has permitted failure envelopes to be plotted. Tension failures dominated the tension-tension domain, while compression failures dominated the compression-compression domain. The tension-compression domain contained a mixture of tension and compression failures.

The use of the biaxial cruciform test data to develop failure criteria provides a clear example of how an experimental technique, allied to suitable analysis tools, can be used to further our understanding of complex composite structures.

INTRODUCTION

Whilst polymer composites, in the form of filament wound tubes, have been tested under multiaxial loading conditions since the mid-1970s, see for example [1-2], resulting in a large body of multiaxial test data, for many aerospace applications, the materials are used in the form of flat or gently curved panels. This makes the use of tubular test specimens unsuitable. For this reason biaxial testing facilities for planar specimens have been developed within QinetiQ and in collaboration with the UK aerospace industry since 1993.

The study discussed in this paper is concerned with the performance of the biaxial stress field around a hole, either left open or filled with a fastener. This latter variant occurs in abundance in structural joints. QinetiQ, formerly referred to as DERA, the Defence Evaluation and Research Agency carried out the research. Test specimens were supplied under a collaborative DTI funded programme intended to develop an understanding of the failure of fibre-reinforced composites under multiaxial loading, as seen in service, and to develop failure prediction techniques for improved cost-effective structural design methods.

Much of the work that has been carried out in the field of biaxial testing has been within the defence and aerospace sectors. While many of the results of the former have now been published, until recently the test data obtained under various multiaxial programmes has been bound by commercial agreements within the aircraft sector and has not been available for release in the public domain. This paper has been written in response to the expiry of one such commercial agreement. As such it discusses the design and manufacture of a series of cruciform specimens

with filled and open holes. The calibration and testing of the specimens is then described in some detail. Biaxial strain ratios were selected for testing purposes that were representative of typical in-service loading. The failure envelopes for the materials are shown and the failure mechanisms are discussed, along with implications for the use of bolts within composite structures.

BIAXIAL SPECIMEN DESIGN AND MANUFACTURE

The experimental programme used a biaxial cruciform specimen designed and validated in a previous programme, [3]. A summary specimens tested within this study is given in Table 1.

Series	Material	t_{test} (mm)	Lay-up
1	T300/914	2.0	$[\{+45, -45, 0, 90\}_4]_S$
2	T300/914	5.0	$[\{+45, -45, 0, 90\}_5]_S$
3	T300/914	5.0	$[\{+45, -45, 0, 90\}_5]_S$
4	T300/914	5.0	$[\{+45/-45/0/0/+45/-45/0/90/0/0\}_2]_S$
5	T300/914 mixed woven	2.0	$[\pm45, 0, 90\}_2]s$

Table 1: A summary of the test specimens investigated, where t_{test} (mm) is the thickness of the test specimen.

The carbon-fibre composite test material was machined to the required geometry, [3] and sandwiched between glass-fibre composite cladding. A circular cut-out in the centre of the cladding, which was tapered to reduce peel stresses, exposed the region of test material to be tested under biaxial loading. Aluminium end-tabs were bonded onto the cruciform for gripping. Holes were drilled through the end-tabbed regions to allow the specimen to be clamped in the test machine grips. The tapers of the specimens to be tested under tension-compression and compression-compression loading were shimmed with an adhesive compound as a means of suppressing buckling. This adhesive compound was sanded level to the glass cladding prior to testing.

Electrical resistance strain gauges were mounted to the surface of the specimens in the configuration shown in Figure 1. A 6mm hole was drilled in the centre of the test region for all except the calibration specimens. Fasteners were inserted and tightened to the specified torque.

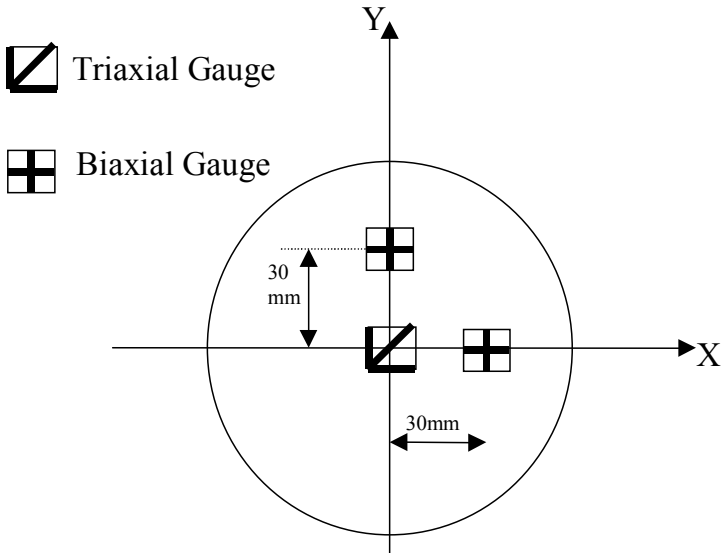

Figure 1: Strain gauge configurations in the exposed test area for the calibration specimens (no central gauge is used in the tests to failure due to the presence of the 6mm hole)

SPECIMEN CALIBRATION

Valid failures of the biaxial cruciform specimens can only be obtained if a hole or other stress-concentrating feature, for example an impact, is contained within the test area. In order to estimate the strain at the centre of the specimen, a calibration procedure is employed that examines the strain at the centre of the specimen, the distribution of the strain across the test area and relates this to the applied loading to obtain stiffness values. Equivalent strains can then be calculated to lie at the centre of the test specimen.

Each specimen was mounted in an anti-buckling guide, prior to being positioned in a purpose built servo-hydraulic biaxial test machine with four 500kN actuators, Figure 2. Load was transferred into the specimen through the bonded end tabs, which were clamped in the grips. The clamping pressure was applied by tightening six bolts that passed through the oversize holes in the end-tabs. The machine was operated in displacement control; load was applied through the application of a displacement on the two axes.

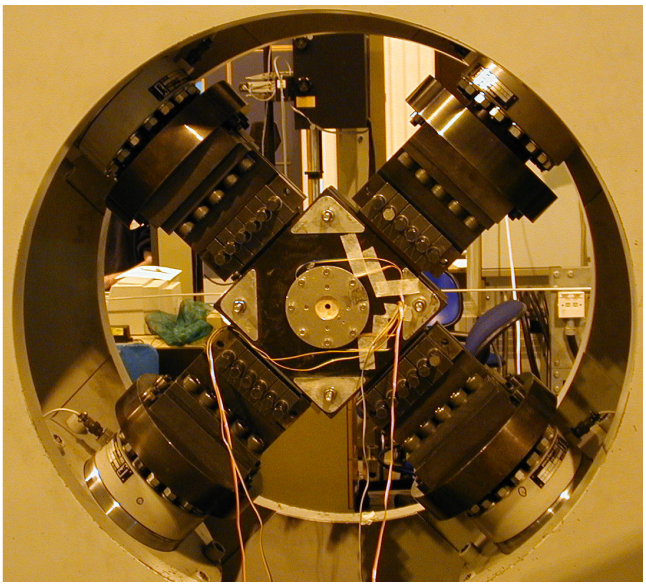

Figure 2: A biaxial cruciform test in progress (note the presence of an anti-buckle guide)

A PC based data-logger was used to record load, displacement, strain and out-of-plane displacement time histories throughout the testing at a frequency of 1Hz.

A summary of the calibration data obtained for all specimens is presented in Table 2 and graphically in Figure 3. LVDTs were used to identify any out of plane displacement that would indicate the presence of buckling. Calibration data was considered to be valid if no evidence of out of plane displacement was obtained and if the strain variation across the test region remained within 10%. It should be noted that the calibration data can only be considered valid up to a predetermined strain level. In the tension-tension quadrant this were typically 6000με; in the tension-compression quadrant this were typically up to 7000με; in the compression-compression quadrant these were typically up to –4000με, Table 2.

For each biaxial strain ratio the specimen compliances (εx/Px) and (εy/Py) were determined, where εx and εx were the measured central strains and Px and Py the loads at the x axis and y axis grips. Strain variation in the test region was calculated from the strain gauge readings at the centre and reference gauges located at a distance from the centre. This data was used to predict the load-strain relationship of the test to failure specimens, Table 3.

Series	Testing ratio	Px (kN)	Py (kN)	εx_cal (με)	εy_cal (με)	Ex (με/kN)	Ey (με/kN)	Buckling strain
1	(+1: +1)	300	295	5619	5637	18.8	19.1	-
1	(+1: +0.5)	264	213	6024	3050	22.7	14.3	-
1	(+1: 0)	242	127	6857	140	28.4	0.6	-
1	(+1: -0.5)	192	5	7571	-3909	38.3	-781.8	-
1	(+1: -1)	117	-111	6921	-7043	58.3	63.9	-
1	(+0.5: -1)	-6	-169	3288	-6794	-548.0	40.0	-6800
1	(0: -1)	-120	-221	-201	-6321	1.7	28.5	-3500
1	(-0.5: -1)	201	-244	-2796	-5485	14.0	22.6	-2500
1	(-1: -1)	171	-171	-3165	-3167	18.7	18.7	-2500
2	(+1: 0)	405	206	5390	-30	13.3	0.1	-
2	(+1: -0.5)	378	-16	7210	-3890	19.1	243.1	-
2	(+1: -1)	185	-199	5469	-5550	29.6	27.9	-
2	(+0.5: -1)	-5	-290	2860	-5430	-572.0	18.7	-
2	(0: -1)	-201	-386	130	-5360	-0.3	13.9	-
5	(+1: +1)	254	257	4550	4550	17.95	17.7	-
5	(+1: -0.5)	198	7	7084	-3698	35.85	-528.3	-
5	(+1: -1)	112	-106	6229	-6389	55.3	61.5	-
5	(+0.5: -1)	-7	-161	2973	-6115	-424.7	38.0	-

Table 2: A summary of the calibration data obtained where D (mm) is the diameter of the test area, Px and Py (kN) is the maximum calibration force, εx_calib and εy_calib are the maximum calibration strains (με) and Ex and Ey (με/kN) are the stiffnesses describing the load-strain relationship up to the maximum calibration strain.

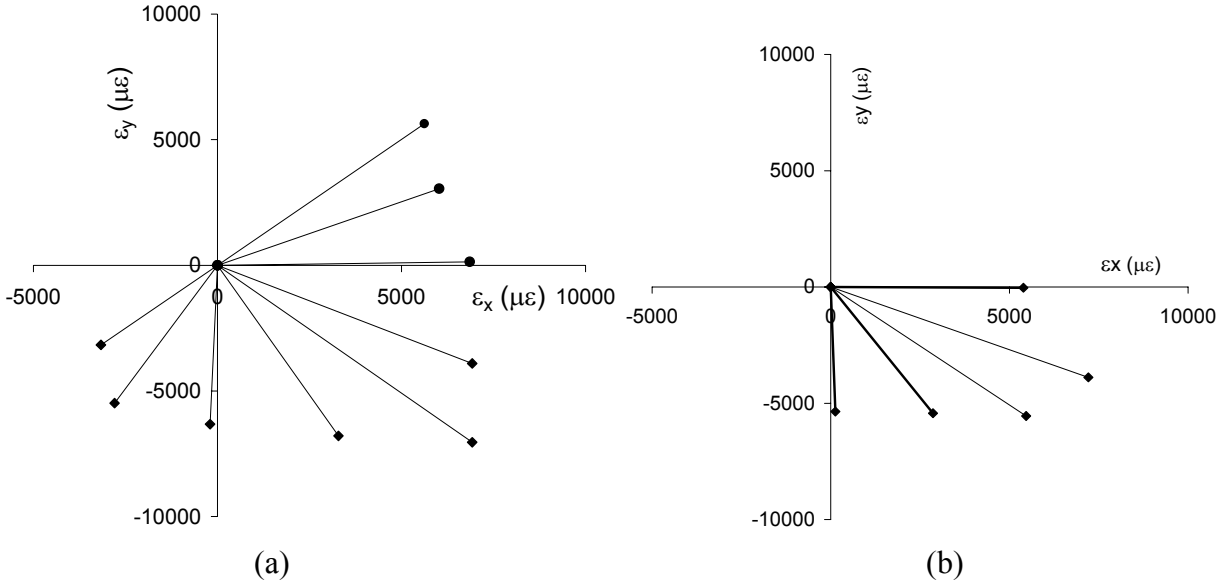

Figure 3: Examples of the calibration data (seies 1, (a),and 2, (b) shown)

TEST TO FAILURE PROCEDURE

The specimens were mounted in the biaxial testing facility as for the calibration tests. The specimens were loaded in displacement control until failure occurred. In the interests of clarity, initial failure is defined as the origin of a deviation from the load-strain time history in excess of

10%. Final failure is assumed to have occurred when the load carrying capacity of the test specimen is reduced by at least 10%. A valid failure was defined as a failure that originated from the centre of the test region if this part of the specimen had not buckled. The reader is reminded that buckling of the test region changes the stress-strain state. For this reason the calibration data would become invalid beyond the point at which any buckling may have occurred. Clearly this invalidates any predicted failure strains, and consequently any predicted failure stresses, beyond this point.

No	Series	Biaxial strain ratio	T (Nm)	Px (kN)	Py (kN)	ε_{x_pred} ($\mu\varepsilon$)	ε_{y_pred} ($\mu\varepsilon$)	σ_{x_pred} (MPa)	σ_{y_pred} (MPa)
1	1	(+1: +1)	6	288	280	5413	5349	401	398
2	1	(+1: +1)	6	295	288	5543	5492	411	409
3	1	(+1: +1)	6	314	310	5897	5918	439	440
4	1	(+1: +0.5)	6	264	214	5993	3065	394	279
5	1	(+1: +0.5)	6	260	207	5897	2958	389	272
6	1	(+1: +0.5)	6	269	217	6111	3108	402	284
7	1	(+1: +0.5)	ft	242	195	5494	2789	361	255
8	1	(+1: +0.5)	ft	257	208	5833	2970	383	271
9	1	(+1: +0.5)	ft	253	203	5732	2908	377	266
10	1	(+1: 0)	6	239	142	6798	85	388	124
11	1	(+1: 0)	6	229	120	6511	72	371	118
12	1	(+1: 0)	6	239	123	6779	74	386	123
13	1	(+1: -0.5)	6	172	4	6583	-3451	313	-80
14	1	(+1: -0.5)	6	166	4	6350	-3278	303	-75
15	1	(+1: -0.5)	6	163	4	6260	-3282	298	-77
16	1	(+1: -1)	6	117	-108	6838	-6926	267	-273
17	1	(+1: -1)	6	123	-112	7178	-7178	282	-282
18	1	(+1: -1)	6	126	-118	7360	-7555	285	-300
19	1	(+1: -1)	ft	120	-114	6987	-7279	269	-291
20	1	(+1: -1)	ft	128	-120	7491	-7692	290	-305
21	1	(+1: -1)	ft	109	-101	6333	-6463	246	-256
22	1	(+0.5: -1)	6	-10	-290	5608	-11589	115	-560
23	1	(+0.5: -1)	6	-10	-287	5553	-11476	114	-554
24	1	(+0.5: -1)	6	-10	-276	5342	-11040	110	-533
25	1	(+0.5: -1)	OH	-7	-195	3768	-7787	77	-376
26	1	(0: -1)	6	-231	-416	-393	-11856	-230	-680
27	1	(0: -1)	6	-205	-372	-348	-10601	-206	-608
28	1	(0: -1)	6	-6	-395	-11	-11250	-198	-639
29	1	(-0.5: -1)	6	-312	-374	-4364	-8459	-230	-328
30	1	(-0.5: -1)	6	-349	-407	-4881	-9189	-159	-223
31	1	(-0.5: -1)	OH	-224	-270	-3129	-6098	-285	-401
32	1	(-0.5: -1)	OH	-219	-263	-3068	-5939	-278	-391
33	1	(-0.5: -1)	OH	-209	-253	-2932	-5709	-267	-376
34	1	(-1: -1)	OH	-259	-260	-4850	-4868	-361	-362
35	1	(-1: -1)	OH	-265	-267	-4956	-4985	-369	-370

3(a): Specimens using series 1 calibration values (OH indicates an open hole specimen)

No.	Series	Biaxial strain ratio	T (Nm)	Px (kN)	Py (kN)	ε_{x_pred} ($\mu\varepsilon$)	ε_{y_pred} ($\mu\varepsilon$)	σ_{x_pred} (MPa)	σ_{y_pred} (MPa)
36*	4	(+1: +0.5)	6						
37	3	(+1: -0.5)	6	324	-13	6195	-3132	297	-69
38*	3	(+1: -0.5)	6	309	-14	5896	-3340	276	-86
39	3	(+1: -0.5)	6	324	-13	6187	-3127	297	-69
40	3	(+1: -0.5)	6	316	-13	6042	-3054	289	-67
41	4	(+1: -0.5)	6						
42	3	(+1: -1)	6	219	-224	6470	-6249	258	-242
43	3	(+1: -1)	6	237	-245	7017	-6844	279	-266
44	3	(+1: -1)	6	234	-233	6934	-6496	280	-247

45	4	(+1: -1)	6						
46[nf]	3	(+0.5: -1)	6	-9	501	4935	9375	116	-446
47[nf]	3	(+0.5: -1)	6	-9	501	4935	9375	116	-446
48	3	(+1: -0.5)	OH	314	-13	6000	-3232	284	-78
49[c]	3	(+1: -0.5)	OH	363	-29	6935	-6943	272	-273
46	3	(+0.5: -1)	OH	-7	-403	3973	-7547	93	-359
47	3	(+0.5: -1)	OH	-7	-405	3984	-7576	94	-360

3(b): Specimens using series 2 calibration values (OH indicates an open hole specimen)

No.	Series	Biaxial strain ratio	T (Nm)	Px (kN)	Py (kN)	ε_{x_pred} (με)	ε_{y_pred} (με)	σ_{x_pred} (MPa)	σ_{y_pred} (MPa)
52	5	(+1: +1)	6	315	316	5653	5603	416	141
53	5	(+1: -0.5)	6	168	6	6012	-3138	290	-78
54	5	(+1: -0.5)	6	179	6	6421	-3351	310	-84
55	5	(+1: -0.5)	6	179	6	6419	-3350	310	-84
56	5	(+1: -1)	6	127	-128	7046	-7865	270	-331
57	5	(+1: -1)	6	125	-119	6900	-7297	271	-301
58	5	(+1: -1)	6	127	-119	7025	-7306	278	-299
59	5	(+0.5: -1)	6	-14	-323	5890	-12261	131	-601
60	5	(+0.5: -1)	6	-14	-321	5860	-12199	130	-598
61	5	(+0.5: -1)	6	-13	-300	5480	-11407	122	-559
62	5	(+1: +1)	OH	305	306	5466	5425	403	401
63	5	(+1: -0.5)	OH	150	5	5378	-2886	260	-70
64	5	(+1: -0.5)	OH	156	6	5596	-2920	270	-73

3(c): Specimens using series 5 calibration values (OH indicates an open hole specimen, ft indicates the bolts were made finger tight)

*Table 3: A summary of the results of the specimens tested to failure, grouped in accordance with the calibration values used. T (Nm) is the applied torque (ft indicates finger tight), Px and Py are the failure loads on the X and Y axes respectively (kN), ε_{x_pred} and ε_{y_pred} are the predicted central strains to failure (με) and σ_{x_pred} and σ_{y_pred} are the predicted central failure stresses (MPa); *indicates an invalid failure, [c] indicates that the cladding was omitted and [nf] indicates that failure was not obtained within the capacity of the test machine.*

EXPERIMENTAL FINDINGS

A summary of the experimental results can be found in Table 3. An example of the resultant failure envelopes can be seen in Figure 4.

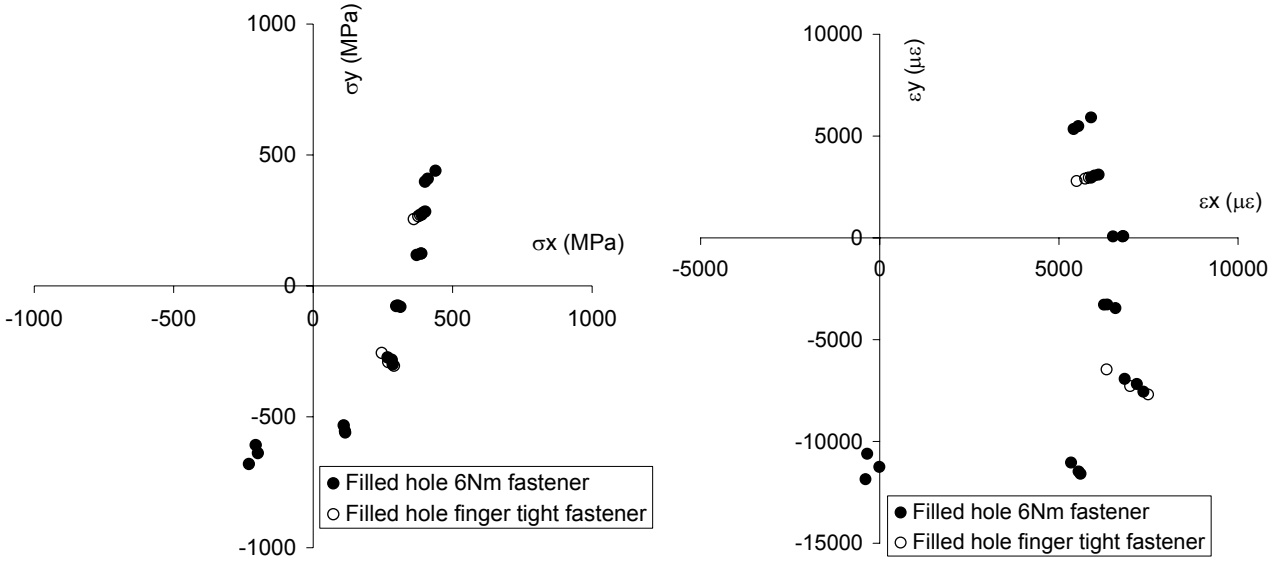

Figure 4: Experimental failure envelopes for 2mm thick T300/914 quasi-isotropic laminates

The predicted failure strain values, ε_{x_pred} and ε_{y_pred}, are the values of equivalent central strain based on the maximum loads, Px (kN) and Py (kN) and the calibration stiffnesses, Ex (με/kN) and Ey (με/kN), given in Table 2. The values of failure stress are calculated values based on the predicted failure strain and laminate theory, assuming the lay-up given in Table 1.

Initial failure was accompanied by acoustic emissions suggestive of damage growth. If evident on the load-strain time histories, this was identified as the failure strain. Final failure of the specimens was obvious in every test: an acoustic emission was clearly heard, accompanied by a sudden drop in load.

Experimental failure envelopes are presented for groups of specimens in Figures 4-6. These failure envelopes, and the results presented in tabular form, suggest good agreement within batches of specimens for the predicted failure strains, typically within a 3%. As these are based on the failure loads and the calibration ratios, this implies that the test procedure developed leads to results that are highly repeatable.

As tensile forces perpendicular to the main axis became more prominent, the failure strain reduced. The failure strain at the strain ratio (+1.0: +1.0) was 80% of the failure strain at (+1: -0.5): the strain ratio comparable to unidirectional tests. At each strain ratio the failure strains were similar for all the different types of 2mm specimens investigated. Compression failures in specimens with filled holes occurred at strains that were of the order of 150% greater than for those with open holes (cf. average values for the (-0.5: -1) ratio, Table 3(a), -4623με with -3043με). It is believed that the bolt prevented hole distortion and thus the compression failures passing through the hole by constraining mechanisms of compressive failure; this in turn induced a secondary tensile failure.

The specimens were all examined using optical and scanning electron microscopy to confirm that they failed in a valid manner, i.e. the failure did not grow from the edge of the specimen, but from within the test area. Cracks were visible in the test regions of all specimens; delamination was visible in the specimens that were tested under compressive loading conditions. The continuity of any cracking on both faces of the panels gave indications of the extent of damage growth prior to catastrophic failure. Typically, the specimens were photographed and sketched to record the appearance of the failure whilst the extent of any delamination was determined using a pulse-echo ultrasonic C-scanning system.

The majority of the failures were valid, with failure originating from the hole without the test region buckling. Some non-linearity of the strain readings that was evident in 2mm thick T300/914 specimens during calibration was attributed to buckling. In tension dominated strain ratios, the failure mechanisms were tensile in nature. In compression-compression ratios, failure mechanisms were compressive in nature. In ratios involving compression and tension strains, there was evidence to suggest that both types of failure had occurred.

The weave pattern of the 5-satin-harness weave fabric only slightly altered the tensile failure mechanism from that observed for the UD material. Furthermore, the woven material prevented compression failure cracking the surface plies.

The central 90° plies were often found to be the site of initiation of failures, see for example Figure 7 for specimen 28. The failure path of specimen 28 passed adjacent to the central hole within the anti-buckling guide, Figure 7(a). Just outside the guide, one of the failure paths diverged to form a Y-shape. The x-ray, Figure 7(b), showed the compressive failure; more splitting was observed than for the specimens tested at the (+0.5 : -1) ratio. The damage under the washer area comprised of compressive damage and 90° splits, but no tensile failure. The damage spread to form many failure paths, some of which reached the edge of the test material.

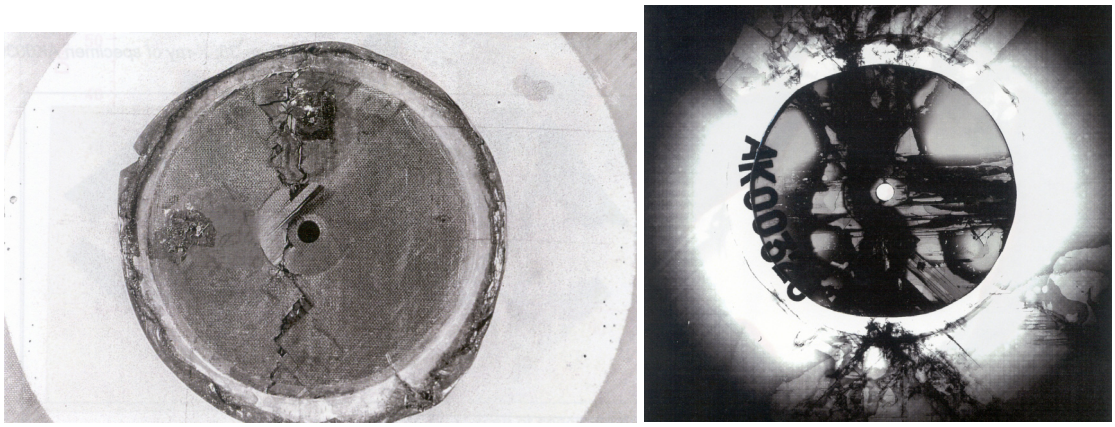

(a) (b)

Figure 7: Surface failures, (a), and X-ray, (b), of specimen 28

IMPLICATIONS OF THE EXPERIMENTAL FINDINGS

The study described herein suggests that current designs of components with notches are conservative.

Measurements made on notched laminates of different lay-ups under biaxial loading at various strain ratios have demonstrated that the capability exists to build up failure envelopes from comparatively few tests.

In the design of notched structures experiencing tension dominated strain ratios, the designer should consider that strains to failure can reduce by up to 20% compared with the failure strains in notched quasi-isotropic uniaxial tests, [4]. In such tension dominated situations, the failure does not appear to be sensitive to the presence of the bolt.

Filled holes can restrict microbuckling of fibres, subsequently giving a higher strain to failure in compression loads. This means that higher design strains, than are currently used, can be sustained if the loading is in compression. However, the extent to which this can be relied on depends on close attention to tolerancing. Thus, designers should consider the implications of fastener fit and tolerance. It is anticipated that the influence of losing a bolt, using a bolt which is too small for the hole, misaligning a bolt, or making the hole larger than was planned would be dramatic in components subjected to extreme compressive loading. That is, in the compression-compression quadrant and at the (+1.0: -1.0) and (+0.5: -1.0) tension-compression strain ratios. It is estimated that the strains to failure would be reduced by up to 50%.

The determination of failure envelopes, combined with fractographic examination of mechanisms, will improve understanding and lead to the development of failure criteria that utilises the material properties with respect to the loading conditions. A review of the extensive amount of work that has been conducted in this area over a considerable number of years was conducted as part of the World Wide failure exercise, [5-11]. These references suggest that while much progress has been made in this area, a universally applicable failure criterion has yet to be established. Work is currently being conducted into providing advice as to suitability and applicability of the various criteria, [12-13]. The intention is to provide designers with guidance on using these criteria in conjunction with Finite Element Analysis to allow damage-tolerant structures to be designed without resorting to over-conservative safety factors. Experimental failure envelopes such as the ones in Figures 4-6 can be used to develop analytical tools for developing failure criteria and addressing problems within composite structure design; for example the optimisation of bolt configurations. In such work it can be assumed that the envelopes are symmetrical about the (+1: +1) – (-1: -1) plane.

THE FUTURE

Clearly the potential benefits arising from the possession of a reliable multiaxial predictive capability are substantial and issues relating to composite structure design are not limited to the aerospace sector; indeed, there is considerable scope for applying the knowledge gained more widely. In the UK, steps are being taken to apply the knowledge gained to other industry sectors under a DTI Funded programme MMS5 - Design and Failure of Materials Systems under Multi-Axial Loads [12]. This programme, which started in September 2002, falls within the DTI's "Measurements for Materials Systems" initiative, [13]. Initially, MMS5 is concerned with addressing the needs of the automotive, shipbuilding, civil engineering, offshore, rail, aircraft and gas sectors, but may well expand further as it progresses. The materials currently under assessment include carbon, glass and aramids and possibly mixtures of these. Woven, braided, tri-axial and discontinuous fibre composites are being assessed, with a distinct move towards the assessment of lower performance bulk usage materials. An important aspect of the programme has been to draw on the findings of the WWFE and apply them to the materials and to solving some of the structural problems that arise. Selected biaxial tests are currently being carried out, both on tubes and cruciforms, as necessary, to establish key data points. In the longer term the guidelines that are developed will be incorporated into national, and, where possible, international standards.

CONCLUSIONS

This paper has presented a number of experimental results from a biaxial testing investigation. These results have been used to establish failure envelopes for a range of laminates containing open and filled holes. A series of recommendations have then been made that impacts of the design and use of bolts within composite structures.

Finally, this paper has highlighted some of the direct benefits that have already been gained through the multiaxial research work that QinetiQ has conducted over the last few years, much of it in conjunction with the DTI and the UK aircraft industry. The biaxial cruciform test has been used to generate representative material and structural performance data on a range of laminates containing structural features such as open and filled holes. This information is being used in the development of analytical tools and the development of predictive failure methods for bolted joints. This provides a clear example of how an experimental technique, closely allied to suitable analysis tools, can be used to further our understanding of complex composite structures.

ACKNOWLEDGEMENTS

The authors would like to acknowledge the DTI and the partners of the multiaxial testing programmes for their considerable and continued support in the field of multiaxial testing and application.

The views expressed in this paper are those of the authors and do not necessarily reflect the corporate views of QinetiQ.

REFERENCES

1. Hinton, M.J., Soden, P.D. and Kaddour, A.S., *"Biaxial failure of composite laminates under combined loads",* Applied Composites Materials, V.3, pp 151-162, 1996.
2. Kaddour, A.S., Soden P.D. and Hinton, M.J., *"Failure of ±55° filament wound tubes under biaxial compression"*, J. Composites Materials, V.32, no.18, pp1618-1645, 1998.
3. Hopgood, P., Cook, J., Clarke, A., *"Multi-axial testing of planar composite specimens",* ICCM12, Paris 1999
4. Kairouz, K, *'Quasi-isotropic lay-up material properties'*, Personal communication kept in DRA file DRA/SMC/6/6/FRN96149, (1997).

5. Hinton, M.J., Soden, P.D., *"Predicting failure in composite laminates: the background to the exercise"*, Composites Science and Technology, V. 58, pp.1001-1010, 1998
6. Hinton, M.J., Kaddour, A.S. and Soden, P.D. *"Failure criteria for FRP's- A world study", (C536-018*), 15-16 Sept 1998, IMechE HQ, London.
7. *FAILURE CRITERIA IN FIBRE REINFORCED POLYMER COMPOSITES: PART A*, edited by Hinton, M.J., Soden, P.D. and Kaddour, A.S., published by Elsevier Science Ltd, 1998.
8. Hinton, M.J., Soden, P.D. and Kaddour, A.S., *"Predicting failure in fibre composites: Lessons learned from the world-wide failure exercise",* Paper 1198, ICCM-13, China, June 2001.
9. Hinton, M.J., Soden, P.D. and Kaddour, A.S., *"Evaluation Of Failure Prediction In Composite Laminates: Background To Part (B) Of The Exercise",* to be published in Compos. Sci. Techno.
10. *PART B: FAILURE CRITERIA IN FIBRE REINFORCED POLYMER COMPOSITES*, Comp. Sci. and Tech., ed. Hinton, M.J., Soden, P.D. and Kaddour, A.S., Elsevier Science Ltd, 2002.
11. *Part C: FAILURE CRITERIA IN FIBRE REINFORCED POLYMER COMPOSITES*, Comp. Sci. and Tech., ed. Hinton, M.J., Soden, P.D. and Kaddour, A.S., Elsevier Science Ltd, 2002.
12. http://www.arpconsortium.org/MMS5/MMS5.htm
13. http://www.npl.co.uk.npl/cmmt/programmes